

# All-optical up-conversion for 2.5-Gb/s signals in ROF systems based on FWM effect in HNLF

Tianliang Wang (王天亮)<sup>1\*</sup>, Hongwei Chen (陈宏伟)<sup>1</sup>, Shizhong Xie (谢世钟)<sup>1</sup>,  
Bouchaib Hraïmel<sup>2</sup>, Luo Ma<sup>2</sup>, and Xiupu Zhang<sup>2</sup>

<sup>1</sup>State Key Laboratory on Integrated Optoelectronics, Tsinghua National Laboratory for Information, Science, and Technology (TNList), Department of Electronic Engineering, Tsinghua University, Beijing 100084, China

<sup>2</sup>ENCS of Concordia University, Montreal, Canada

\*E-mail: wtl04@mails.tsinghua.edu.cn

Received April 17, 2010

We propose and demonstrate experimentally a novel scheme to realize all-optical up-conversion and wavelength-conversion based on the bi-directional-pump four-wave mixing (FWM) effect in high nonlinear fibers (HNLFs). The pump is generated with optical carrier suppression in a Mach-Zehnder modulator. The two pumps are always parallel and phase-locked. A balance-detection photo-detector for optical signal detection is employed with 3-dB improvement in power penalty. The 2.5-Gb/s signals are transmitted successfully over the 25-km single-mode fiber in 30-GHz radio over fiber (ROF) systems.

OCIS codes: 060.4370, 060.5625.

doi: 10.3788/COL20100811.1037.

Radio over fiber (ROF) is a good candidate for broadband wireless multimedia access network because of its immunity to electro-magnetic interference and its capability of providing high-bandwidth-access services for mobile communications, wireless large-area networks, and fixed wireless-access services, such as local multi-point distribution systems. All-optical frequency up-conversion, a process employed in generating optical radio frequency signals, is a key technique in ROF systems<sup>[1–10]</sup>. Up-conversion schemes utilizing optical nonlinearities, such as cross-gain and cross-phase modulations in nonlinear materials, have been investigated. Polarization-sensitive all-optical up-conversion methods based on external intensity and the phase modulator have been demonstrated<sup>[9,10]</sup>, respectively. Another scheme to accomplish all-optical up-conversion is by using cross-absorption modulation in an electro-absorption modulator (EAM)<sup>[1–5]</sup>. However, these up-conversion techniques have some drawbacks, such as limited frequency response, conversion loss, and sensitivity to polarization of optical signals. Yu *et al.* proposed a scheme for all-optical up-conversion using four-wave mixing (FWM) in high nonlinear fibers (HNLFs)<sup>[6]</sup>. In their setup, the optical carrier sidebands of the signals were suppressed by the optical filter (25/50 GHz interleaver), and the efficiency of the light source decreased.

In this letter, we propose an all-optical up-conversion and wavelength conversion scheme based on FWM in HNLF. Co-polarized pump light waves were generated by the optical carrier suppression (OCS) modulation technique with the use of a laser. As FWM is independent of signal bit rates and coding formats<sup>[2–4]</sup>, it can be used to realize up-conversion and wavelength conversion in high bit rate and complex signals with low-frequency bandwidth (i.e., for optical and electrical components) and high wavelength stability. Compared with Ref. [6], this letter offers some novel concepts and findings: 1) the use of idlers to pump 30-GHz signals; 2) provision of counter-propagating signal waves as an alternate to

the optical filter; and 3) the use of all the sidebands generated by FWM to improve optical source efficiency and the detection of optical signals by balance-detection photo-detector with 3-dB improvement in power penalty.

The schematic diagram of the system is shown in Fig. 1. Microwave signal was applied to the LiNbO<sub>3</sub> Mach-Zehnder modulator (LN-MZM) biased by a suitable voltage to suppress the optical carrier from the laser source to its maximum. The two first-order sidebands at the output of the MZM acted as optical pump sources and were sent to the HNLF. The optical signal sources at the output of the intensity modulator were simultaneously sent to the HNLF from the inverse direction for down-link data up-conversion. Optical output was sent to the balance-detection photo-detector after the 25-km single-mode fiber (SMF). The detected signal was measured by a bit error rate tester (BERT).

We assumed that the phase noise of the input light was  $\psi_0(t)$  and the phase noise of the electronic signals was  $\varphi_0(t)$ . The bias voltage of the LN-MZM was tuned

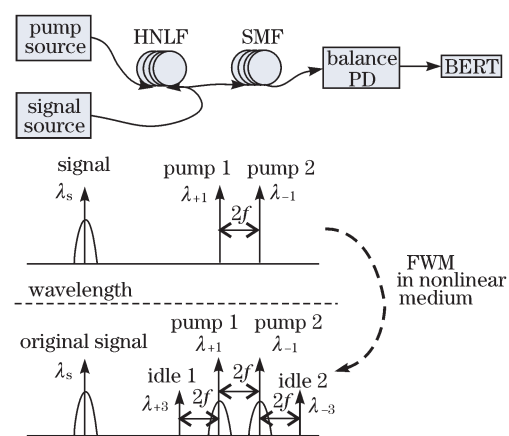


Fig. 1. All-optical up-conversion and wavelength-conversion in the ROF system. PD: photodiode.

such that it suppresses all even-order optical sidebands,  $V_B = V_\pi$ ,  $V_B$  is the bias point of the modulator, and  $V_\pi$  is the half-wave voltage of the modulator, in accordance to the origin of OCS modulation. The field of the output light is

$$\begin{aligned} E_{\text{out}}(t) &\approx J_1(\beta)E_o\{\cos[(\omega_o - \omega_e)t + \varphi_0(t) - \varphi_0(t) - \phi] \\ &\quad + \cos[(\omega_o + \omega_e)t + \psi_0(t) + \varphi_0(t) + \phi]\} \\ &= J_1(\beta)E_o\{\cos[\omega_{-1}t + \varphi_{-1}(t) - \phi] \\ &\quad + \cos[\omega_{+1}t + \varphi_{+1}(t) + \phi]\}, \end{aligned} \quad (1)$$

where  $E_o$  is the electric field amplitude,  $\omega_o$  is the optical carrier frequency,  $\omega_e$  is the drive frequency, and  $\phi$  is the phase of the electrical signal. The frequencies of the outputs of the modulator biased on  $V_\pi$  are given by

$$\omega_{\pm 1} = \omega_o \pm \omega_e. \quad (2)$$

The first-order sidebands produced by LN-MZM acted as two pump waves, which were sent to the HNLf. The optical signal sources at the output of the intensity modulator were simultaneously sent to the HNLf from the inverse direction. According to the theory of FWM<sup>[3]</sup>, the pump waves and the signal light mix and create new idle wavelength lights,  $\lambda_{+3}$  and  $\lambda_{-3}$  (i.e., the frequencies are  $\omega_{+3}$  and  $\omega_{-3}$ ) (Fig. 1). The frequencies of the new idle wavelength are given by

$$\omega_{\pm 3} = 2\omega_{\pm 1} - \omega_{\mp 1} = \omega_o \pm 3\omega_e. \quad (3)$$

The millimeter wave (mm-wave) generated by beating between  $\lambda_{+1}$  and  $\lambda_{-3}$ , as well as between  $\lambda_{+3}$  and  $\lambda_{-1}$ , was used for the 2.5-Gb/s data up-conversion based on FWM effect of the HNLf in the ROF system.

The experimental setup for the proposed ROF system is illustrated in Fig. 2. At the central station, the continuous wave (CW) light was generated by a laser diode (LD) at 1552 nm, passed to a dual-arm LN-MZM biased on  $V_\pi$ , and driven by a complementary 7.5-GHz microwave source. The optical pump sources at the output of the MZM were then sent to HNLf, and the optical signals sources with a wavelength of 1549 nm at the output of the intensity modulator were sent simultaneously to the HNLf from the inverse direction. It concurrently generated the optical mm-wave and up-converted

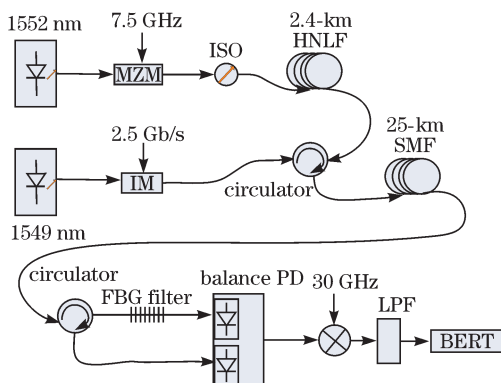


Fig. 2. Experimental setup delivering 2.5-Gb/s downlink services using FWM effect for all optical up-conversion. IM: intensity modulator; ISO: isolator; LPF: low pass filter; PD: photodiode.

the 2.5-Gb/s pseudo-random binary sequence (PRBS) data into an optical mm-wave signal. The conversion was based on the FWM effect in the HNLf. After transmission over various lengths of SMF, the optical mm-wave carrying the 2.5-Gb/s signals was amplified to 10 dBm by an erbium-doped fiber amplifier (EDFA) with a 30-dB small-signal gain. The four optical sidebands (i.e.,  $\lambda_{+3}$ ,  $\lambda_{+1}$ ,  $\lambda_{-1}$ , and  $\lambda_{-3}$ ) were then separated by the FBG filter to determine  $\lambda_{+1}$  and  $\lambda_{-3}$ , as well as  $\lambda_{+3}$  and  $\lambda_{-1}$ , for balance detection. It would be more stable and efficient if an interleaver is employed for selecting the required wavelengths<sup>[7]</sup>. Before detection, the signal was filtered by a 1.0-nm bandwidth tunable optical filter for the amplified spontaneous emission noise reduction. Direct detection was made by a 40-GHz bandwidth balance positive-intrinsic-negative (PIN) photodiode (PD). The demodulated signals were then measured by BERT. In real network applications, a diplexer connected to an antenna acts as a circulator. This is used to handle the upstream and downstream signals.

The powers of the optical sources (1552 and 1549 nm) were both set at 10 dBm. Figure 3(a) shows the optical spectrum obtained directly after OCS modulation. The carrier suppression ratio was around 30 dB, and the frequency difference of the generated optical local oscillator signal was 15 GHz. Figure 3(b) shows the optical spectrum of the optical signal sources before reaching the HNLf. The HNLf was with 2.4-km length, zero dispersion wavelength at 1310 nm, dispersion slope of 0.02 ps/(nm<sup>2</sup>·km), loss of 0.4 dB/km, and nonlinear coefficient of 10 W<sup>-1</sup>·km<sup>-1</sup>. The optical FWM spectrum at the output end of the HNLf (i.e., after the optical circulator) is shown in Fig. 3(c). The generated idler light waves by the FWM effect refer to the two third-order

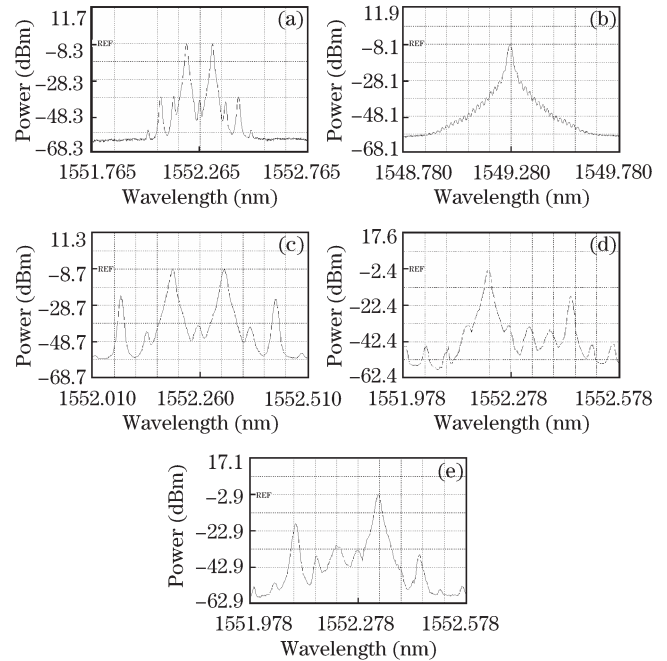


Fig. 3. Optical spectra (bandwidth: 0.01 nm). (a) Optical pump source before the HNLf; (b) optical signal source before the HNLf; (c) after the HNLf; (d) transmitted sidebands of the FBG optical filter; (e) reflected sidebands of the FBG optical filter.

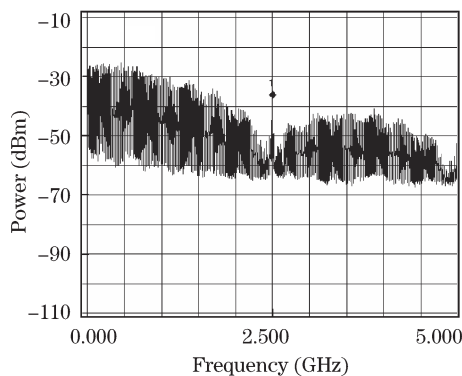


Fig. 4. Electrical spectrum after the balance-detection photo-detector.

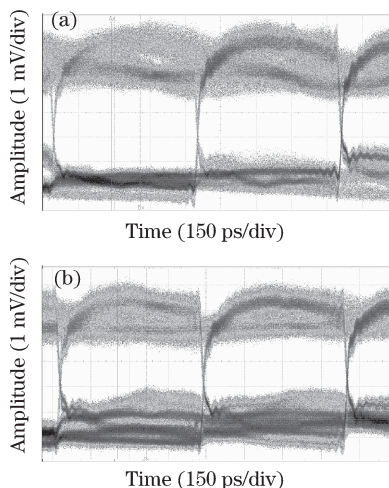


Fig. 5. Eye diagrams (a) after demodulation by an electric mixer in back-to-back configuration and (b) after transmission over 25-km SMF.

sidebands, which are 17 dB lower than the first-order sidebands. Figures 3(d) and (e) show the transmitted and reflected sidebands of the FBG optical filter, respectively.

The carrier suppression ratio was over 30 dB, and the frequency of the generated optical local oscillator signal was 30 GHz. Despite an overall good agreement between theoretical analysis and experimental results, a difference in the spectra of the even-order sidebands power level was observed. The measured higher power level was due to the imperfect control of the delay needed to obtain the LN-MZM complementary driving signals performing the OCS modulation. The exact bias voltage from the theoretical analysis provided better suppression of even-order (zero and second) sidebands, resulting in higher dispersion tolerance. As the FWM effect in HNLFF created a spectrum with two peaks separated by 30 GHz, the mm-wave suffered from chromatic dispersion impairments throughout its propagation in the SMF.

Figure 4 shows the result of the demodulated radio frequency spectrum after 25-km propagation in the SMF. The frequency of the microwave source was set to 7.50 GHz. The 30-GHz harmonics (i.e., quadruple microwave harmonic) with power of around  $-20$  dBm of the microwave driver signal were obtained. The 2.5-Gb/s PRBS

data were up-converted into this optical mm-wave signal.

Figures 5(a) and (b) show the optical eye diagrams in back-to-back configuration and after 25-km propagation in SMF, respectively. After 25-km downlink transmission, the quality factor ( $Q$ -factor) of the eye diagram decreased from 8.5 to 6.5. The decreased  $Q$ -factor and the signal power fluctuations increased with chromatic dispersion. As far as the 2.5-Gb/s signal is concerned, the difference between experimental and theory analyses was caused by setup imperfections. In particular, the OCS, which is considered perfect in theory analysis, did not produce exact and stable optical carrier suppression, affecting overall performance. Figure 5 shows that the downlink data is successfully transmitted through the 25-km SMF with a  $Q$ -factor of over 6. Optical signals were detected by balance-detection photo-detector with a 3-dB improvement in power penalty.

In conclusion, we propose and demonstrate experimentally a novel ROF scheme providing 2.5-Gb/s downlink services. This approach generates mm-wave signals (30 GHz) of quadruple microwave source frequency (7.5 GHz), up-converting simultaneously the signals by using FWM in HNLFF. For the 30-GHz mm-wave up-conversion in the downlink, OCS demonstrates unique advantages in terms of system simplicity and transmission performance. Downlink data are transmitted successfully through 25-km SMF with a  $Q$ -factor of over 6. Experimental results agree with results from theoretical analysis, showing that this architecture is a feasible solution for future optical-wireless access networks, as it offers high degree of scalability.

This work was supported by the Tsinghua Basic Research Fund (No. JC2007020), the National Natural Science Foundation of China (Nos. 60736002 and 60807026), the National "863" Program of China (Nos. 2007AA01Z264 and 2006AA01Z237), and the National "973" Program of China (No. 2006CB302806).

## References

1. Q. Xu, Q. Ye, Z. Pan, Z. Fang, H. Cai, and R. Qu, *Chin. Opt. Lett.* **8**, 7 (2010).
2. H. Yang, J. Sun, and Q. Du, *Chinese J. Lasers* (in Chinese) **36**, 1448 (2009).
3. T. Jiang, D. Huang, X. Zhang, Q. Zhang, and J. Wang, *Acta Opt. Sin.* (in Chinese) **28**, 36 (2008).
4. C. Xie, B. Zhang, X. Lai, and Y. Su, *Chinese J. Lasers* (in Chinese) **36**, 846 (2009).
5. A. Hamié, A. Sharaiha, M. Guégan, and J. L. Bihan, *IEEE Photon. Technol. Lett.* **17**, 1229 (2005).
6. J. Yu, M.-F. Huang, Z. Jia, L. Chen, J.-G. Yu, and G.-K. Chang, *J. Lightwave Technol.* **27**, 2605 (2009).
7. J.-H. Seo, C.-S. Choi, Y.-S. Kang, Y.-D. Chung, J. Kim, and W.-Y. Choi, *IEEE Trans. Microw. Theory Tech.* **54**, 959 (2006).
8. M. Ogusu, K. Inagaki, Y. Mizuguchi, and T. Ohira, *IEEE Trans. Microw. Theory Tech.* **51**, 382 (2003).
9. J. J. V. Olmos, T. Kuri, and K. Kitayama, *J. Lightwave Technol.* **25**, 3374 (2007).
10. Z. Jia, J. Yu, D. Boivin, M. Haris, and G.-K. Chang, *IEEE Photon. Technol. Lett.* **19**, 653 (2007).